CONF-801011--51

LA-UR-80-2926

TITLE: NUCLEONIC ANALYSIS OF A PRELIMINARY DESIGN FOR THE ETF NEUTRAL-BEAM-INJECTOR DUCT SHIELDING

MASTER

AUTHOR(S): W. T. Urban
T. J. Seed
Donald J. Dudziak

SUBMITTED TO: Fourth Topical Meeting on The Technology of Controlled Nuclear Fusion, October 14-17, 1980, King of Prussia, PA

University of California

LOS ALAMOS SCIENTIFIC LABORATORY
Post Office Box 1663 Los Alamos, New Mexico 87545
An Affirmative Action/Equal Opportunity Employer

Form No. 836 R3
St. No. 2629
12/78

UNITED STATES
DEPARTMENT OF ENERGY
CONTRACT W-7405-ENG-36

NUCLEONIC ANALYSIS OF A PRELIMINARY DESIGN FOR THE ETF NEUTRAL-BEAM-INJECTOR DUCT SHIELDING

W. T. Urban, T. J. Seed, and Donald J. Dudziak
Theoretical Division, Los Alamos Scientific Laboratory,
Los Alamos, New Mexico 87545

SUMMARY

A nucleonic analysis of the Engineering Test Facility Neutral-Beam-Injector duct shielding has been made using a hybrid Monte Carlo/discrete-ordinates method. This method used Monte Carlo to determine internal and external boundary surface sources for a subsequent discrete-ordinates calculation of the neutron and gamma-ray transport through the shield. The analysis also included determination of the energy and angular distribution of neutrons and gamma rays entering the duct from the torus plasma chamber. Confidence in the hybrid method and the results obtained was provided through a comparison with three-dimensional Monte Carlo results.

INTRODUCTION

The Engineering Test Facility (ETF) conceptual shields for the Neutral-Beam-Injector (NBI) and the Vacuum-Pumping Duct are being analyzed through the marriage of a three-dimensional (3-D) Monte Carlo calculation with a two-dimensional (2-D) discrete-ordinates calculation. Figure 1 is a schematic illustrating the geometrical relationships of these ducts to the ETF torus and to one another. Presented herein are the results of the analysis of the NBI duct and its shielding. A more detailed description of the NBI duct analysis as well as the vacuum duct will be contained in a forthcoming report[1].

Evaluation of the NBI duct and shielding requires first that an accurate knowledge of the neutrons and gamma rays entering the NBI duct be available. For this reason the geometry considered in the NBI analysis must include the toroidal plasma chamber and associated inboard and outboard shields as well as the NBI duct and its shielding. Furthermore, it is recognized that the shield thicknesses, compositions, and sizes of the ducts are conceptual at this stage of the design and subject to change. The parameters used in this analysis represent the best available at the initiation of this effort, at which time they were frozen.

The analysis of large ducts and their associated shielding is consistently a problem.[2] Although deterministic methods such as discrete ordinates can easily provide the desired pointwise responses at deep penetrations within a shield, they are hampered by ray effects associated with streaming down ducts and their geometry limitation. On the other hand, Monte Carlo methods can readily handle 3-D geometries and streaming down ducts but cannot reasonably provide pointwise responses over an entire shield. The approach taken here has been to marry the two methods in such a manner as to take advantage of the strong points of each method.

Conceptually, the application of a hybrid Monte Carlo/discrete-ordinates method is straightforward. Simply stated, with regard to the NBI duct analysis, Monte Carlo was used to determine a spatially, angularly, and energy dependent source distribution of neutrons and gamma rays incident on the NBI duct walls. This incident flow of radiation was then transformed to a surface source for use in a 2-D discrete-ordinates calculation to obtain the spatially dependent fluxes throughout the shield.

Three-dimensional calculations were performed using the continuous-energy Monte Carlo code MCNP[3] and 2-D calculations were performed using the triangular mesh discrete-ordinates code TRIDENT-CTR.[4] Both codes are avialable to the fusion community through RSIC and the NMFECC.

CALCULATIONAL PROCEDURE

A number of calculational steps were undertaken in this analysis. In order to provide an overview, for the following more detailed discussion, these steps are listed below.

1. An MCNP calculation was made using only the torus geometry and included the inboard and outboard shields as well as the duct penetration through the outboard shield. From this calculation the energy and angular dependent neutron and gamma-ray flow entering the NBI duct and incident on the outboard shield first wall adjacent to the NBI duct was obtained.

2. Using the results from 1 to define a surface source at the NBI duct mouth, an MCNP calculation was performed to determine the spatially dependent energy and angular distribution of neutrons and gamma rays incident on the duct walls. Since no transport in the duct shielding was considered this calculation was essentially one of ray-tracing.

3. The neutron and gamma-ray flow incident on the torus outboard shield from 1 and that incident on the duct walls from 2 were used to generate boundary and internal surface sources for an (R,Z) geometry TRIDENT-CTR calculation to obtain the neutron and gamma-ray flux distributions throughout the NBI shield.

4. Using the flow of neutrons and gamma-rays incident on the torus outboard shield and entering the NBI duct from 1, MCNP calculations were made to obtain the neutron flux in the duct and also selected responses in the NBI shielding for comparison with the TRIDENT-CTR results.

MCNP MODELS AND CALCULATIONS

The configuration of Fig. 1 was broken into three distinct geometrical segments to facilitate acquisition of the required information and to minimize the duplication of the calculational effort. Segmentation was accomplished, from a calculational viewpoint, through the use of trapping surfaces. When a particle crosses a trapping surface its spatial coordinates, direction cosines, energy, weight and time are written to tape. The MCNP calculation can then be continued with the trapped particle information being used to define a secondary source plane. For the problem at hand a trapping surface was located at the torus outboard shield first wall at and around the NBI duct. The azimuthal symmetry of the torus was used to good advantage to reduce the variance of the trapped particles.

Figures 2 and 3 are elevation and plan views of the torus MCNP model. The outboard shield consisted of 0.3 m of stainless steel followed by 0.9 m of a homogeneous mixture of stainless steel and borated water. The inboard shield consisted of 0.02 m of carbon armor, 0.205 m of stainless steel and 0.615 m of a homogeneous mixture of stainless steel and borated water. In both shields the homogeneous mixture consisted of 70 v/o stainless steel and 30 v/o borated water (2 atom/o ^{10}B).

The plasma was represented as a uniformly distributed source of 14-MeV (2.25-pJ) neutrons which were produced with an isotropic angular distribution. This source was "D" shaped in cross section with its axis of revolution congruent with the toroidal axis. Normalization of the source was such as to represent a volumetric source strength of 1.38×10^{18} plasma neutrons/m^3 s. This normalization results in an incident neutron energy flow rate on the outboard shield due to neutrons with energies between 13.5 and 15.0 MeV of ~ 2.4 MW/m^2.

MCNP was run in a coupled neutron/gamma-ray mode and all cross sections were taken from the MCNP Recommended Monte Carlo Cross-Section (RMCCS) Library[3]. A standard LASL 42 energy-group structure was used in the edits, and consisted of 30 neutron and 12 gamma-ray energy groups.

Approximately 2 hours of CDC-7600 time was required to track 120 000 source neutrons. From this run, 122 372 trapped neutrons and 19 568 trapped gamma rays were written to tape for subsequent use in the NBI duct analysis.

MCNP calculations for the NBI duct and shielding used the geometry shown in Fig. 4. The purpose of these calculations was two-fold: (1) to obtain data from which a surface source for use with TRIDENT-CTR can be constructed, and (2) to allow an intercomparison of Monte Carlo and TRIDENT-CTR results at selected locations in the NBI duct and shield and to trap neutrons and gamma rays entering the vacuum duct.

For the calculations to obtain a surface source for TRIDENT-CTR, no transport of radiation in the shield was considered; i.e., once a particle had crossed into the duct shielding it was terminated. Radiation crossing each of the duct wall surfaces was binned by spatial segment into energy and angular bins. Fifteen angular bins corresponding to an S_{16} angular quadrature

was used. The 3-D (energy, angle and one spatial direction) binning on each of the four duct walls required that a large number of particles be started to ensure reasonable statistics in each differential element. To circumvent running large numbers of particles in the torus calculation to get a sufficient number of trapped neutrons at the entrance to the NBI duct, the trapped neutrons were used to construct semi-analytic source angular distributions at the duct mouth. Because of the similarity of the angular distributions at low energies it was found that only two angular distributions were required for the neutrons entering the duct; i.e., one for neutrons with $E > 13.5$ MeV and one for neutrons with $E \leq 13.5$ MeV. The gamma-ray angular distribution can be well approximated by the $E \leq 13.5$ MeV neutron angular distribution.

Two MCNP calculations were made using these semi-analytic source angular distributions at the duct mouth. In each case 250 000 neutrons were started, requiring ~ 12 minutes of CDC 7600 time. Following each calculation, the data for the four duct walls were averaged to obtain a single spatially dependent angular distribution. The resulting average data, together with the appropriate neutron and gamma-ray energy distributions, provided the basis for the NBI duct wall surface source for TRIDENT-CTR; i.e., internal boundary source.

To obtain results which could be compared with the TRIDENT-CTR results at selected locations, another MCNP calculation was made, but this time transport was allowed in the NBI duct shielding. Figure 4 is the MCNP geometry used in this calculation. In this model the duct shielding nearest to the torus was 0.8-m thick and consisted of 0.2 m of stainless steel and 0.6 m of a homogeneous mixture of stainless steel and borated water. The thinner portion of the NBI shield is 0.5-m thick and consisted of 0.125 m of stainless steel and 0.375 m of a homogeneous mixture of stainless steel and borated water. The homogeneous mixture described here is identical in composition to that described earlier for the torus outboard shield.

In this model the tapered NBI duct shield has been approximated by stepping the shield. This simplication does not significantly affect the comparison of the MCNP results to the TRIDENT-CTR results, which used tapered shields, because the regions considered for comparison were chosen such that the average MCNP shield at these points closely approximated the tapered TRIDENT-CTR shields. The MCNP model did contain the vacuum duct penetration of the NBI duct shield which is not in the TRIDENT-CTR model.

In this calculation the trapped neutrons were used as the surface source at the NBI duct mouth. Biasing of the calculation was such as to reduce variance of the neutron flux at the regions of interest for comparison with TRIDENT-CTR. In addition, this calculation provided the trapped neutrons and gamma-rays at the NBI duct/vacuum-pumping duct interface which are being used to evaluate the vacuum duct shielding. The 122 372 trapped neutrons were followed at a time expenditure of ~ 4.5 hours of CDC 7600 time.

A similar calculation was made using the trapped gamma rays, from the torus calculation, as the surface source at the NBI duct mouth. This calculation allows one to ascertain, quantitatively, the importance of the torus gamma rays to the NBI duct shield and streaming down the duct. A total of ~ 4 minutes of CDC 7600 time was required for this calculation.

TRIDENT-CTR MODEL AND METHOD

TRIDENT-CTR calculations were performed on a simplified model of the NBI duct to generate spatially detailed neutron and gamma-ray fluxes. These fluxes are required for the calculation of design analysis parameters such as shutdown dose rates, heating rates and others. In order to pose the original NBI duct problem in a form amenable to solution by TRIDENT-CTR, the duct was modeled as shown in Fig. 5.

The rectangular cross section of the duct was approximated by a circular cross section of the same area, with the width of the duct shielding set to the design specifications. The problem was modeled in (R,Z) geometry with the Z axis running down the center of the NBI duct and the R axis traversing the duct shielding. Because of the triangular mesh feature of TRIDENT-CTR it was possible to more easily model the duct shield taper and the shutter shield within the limitations of a 2-D geometry. The function of the rotating stainless steel shutter shield is to shield the NBI chamber after plasma ignition. The shutter shield was modeled in the open position for this calculation. The spatial mesh for the model as shown in Fig. 5 was laid out on 62 bands with a total of 1 948 triangles.

The cross-section set used was derived from the standard LASL 30 x 12 MATXS Library[5] using the TRANSX code[6]. The scattering order used was P_3 with the cross sections transport corrected using the Bell, Hansen, and Sandmeir methodology[7]. Group-dependent

quadrature sets were used with the S_4, S_6, S_8 and S_{10} EQ_N sets being used in various energy groups.[8] The highest S_N orders were used in those enery groups with the highest portion of incoming source.

In order to bypass the neutron streaming problems that the discrete-ordinates methodology would have encountered in transporting the incoming source from the mouth of the duct toward the NBI chamber, the source at the mouth of the duct was replaced by an incoming internal boundary source along the inside surface of the duct shield. The source was generated by the Monte Carlo code MCNP and given for an S_{10} quadrature set along the length of the duct, as has been previously described. Two angle-space shapes were given with a 42-group spectrum. One shape was for E > 1.35 MeV neutrons and the other shape was for both $E \leq 13.5$ MeV neutrons and gamma rays. A code was written to interpolate the MCNP data onto the TRIDENT-CTR spatial mesh and varying quadrature structure.

The problem was run on the CDC-7600 at the NMFECC in approximately 70 minutes. Several regions of the problem were edited for comparison with the MCNP results.

RESULTS

The calculations described have yielded a considerable amount of information concerning the neutron and gamma-ray populations and transport in the NBI duct as well as the flow of this radiation into and out of this duct. Presentation of all available information here is not possible and therefore a representative sampling of the results pertaining to the NBI duct and its shielding follows. Those interested in more detailed results (e.g., groupwise data and angular distributions) for the NBI duct as well as the forthcoming vacuum duct analysis, are directed to Reference 1.

Presented in Figure 6 is the neutron spectrum for the flow of neutrons into the NBI duct and also incident on the outboard shield in the vicinity of the outboard shield first wall/NBI duct interface (i.e., the trapping surface) as determined by MCNP. This spectrum is normalized to one neutron. It is noted that approximately 25% of the neutrons have energies between 13.5 and 15.0 MeV and approximately 69% have energies less than 1.353 MeV. The majority of this spectral data have fractional errors (i.e., relative standard deviations) of less than 5%, with the intergrated spectrum having a fractional error of less than 0.5%. Fractional errors quoted above and throughout this discussion are at the 68% confidence level.

The angular distribution of these neutrons is illustrated in Fig. 7 for two energy groups (i.e., E > 13.5 and $E \leq 13.5$ MeV) wherein the relative number of neutrons is plotted versus cosine(theta). Theta is the angle between the normal to the torus outboard shield first wall/NBI duct interface (i.e. the trapping surface) and the neutron direction. In examining this figure the reader is cautioned to note that for cosine(theta) greater than 0.5 the bin width is one-half of what it is for cosine (theta) less than 0.5. Thus, the angular distribution for neutrons of $E \leq 13.5$ MeV is a monotonically increasing function of cosine(theta). The E > 13.5 MeV curve decreases slightly and then levels off above cosine(theta) equal to 0.8. This decrease and leveling off results from the position of the inboard shield relative to the duct; i.e., the inboard shield effectively decreases the plasma volume having a line-of-sight path to the duct. The angular data for $E \leq 13.5$ MeV have fractional errors of less than 2% except when cosine(theta) is less than 0.2, when the fractional errors are still less than 5%. For the E > 13.5 MeV data, the fraction errors are less than 5% for cosine(theta) greater than 0.3 and become sufficiently high as to make the data unreliable below cosine(theta) equal to 0.2.

TRIDENT-CTR contour plots of the total (integrated over all energies) neutron flux and total (neutron and gamma-ray) heating are presented in Figures 8 and 9, respectively. Figure 10 is a blowup of the neutron flux in the vicinity of the shutter. The stepped boundary on the right hand side of the contour plots is the result of overlaying the tapered shield boundary of the TRIDENT-CTR model with a rectangular plotting grid. The TRIDENT-CTR neutron flux values in the duct do not include either the tracklength for neutrons prior to their first incidence on the duct wall, or the tracklength for neutrons which travel in the duct from the plasma chamber to the NBI chamber without having an interaction with the duct shielding. The reason for this is that the generation of the internal boundary source was based on only those neutrons incident on the duct walls. Routines for using TRIDENT-CTR data to generate 30-color contour plots have also been developed. Such color contour plots were made for the results of this calculation but could not be incorporated in this paper because of color reproduction limitations.

The neutron flux falloff down the NBI duct as obtained from the MCNP calculations is presented in Fig. 11 for both neutrons with energies greater than 13.5 MeV, and the total over all energies. These fluxes represent those neutrons which scatter from

the duct shielding plus those which stream down the duct without interaction in the duct shield. The fractional error varied from 1.15% to 7.75% for the E > 13.5 MeV flux and from 0.46% to 2.53% for the total flux.

A comparison of the hybrid MCNP/TRIDENT-CTR calculation to the all MCNP calculation is given in Table I. Locations for the regions used in this comparison are indicated in Fig. 4. In general, the comparison between the two methods is quite good. The region III results are, however, somewhat different from the others in that the TRIDENT-CTR flux is lower and the heating much higher than the corresponding MCNP results. At present a quantitative explanation for this anomaly is not available, but it is believed to be, in part, a result of several factors including the perturbation introduced by the vacuum duct penetration which is contained in the MCNP model and not in the TRIDENT-CTR model, geometric differences between the cylindrical and rectangular shield models and differences in the borated water cross sections used by the two codes. It should also be noted that the gamma rays produced in the torus shield have little impact on the NBI shielding as evidenced by the fact that in region I these gamma rays contribute only $\sim$ 8% of the total heating and are a negligible contributor to the region II total heating.

This comparison provides confidence in the NBI duct shield analysis performed and the results obtained. Furthermore, it provided assurance as to the validity of the hybrid MCNP/TRIDENT-CTR method used and demonstrated the applicability of such an approach to the analysis of full scale design problems. The vacuum duct analysis currently underway will hopefully provide further confidence in this hybrid methodology and also additional insight as to how the procedure for linking the two codes can be generalized and more fully automated.

CONCLUSIONS

The analysis has demostrated that a marriage of MCNP and TRIDENT-CTR (i.e., Monte Carlo and discrete ordinates) can be used in full scale design applications for the analysis of large duct shields. The validity of this procedure was provided through comparison with 3-D MCNP results. Although currently existing Monte Carlo and discrete-ordinates codes were used in the analysis, special purpose routines were written to facilitate linkage of the two codes. Codes for linking Monte Carlo and discrete ordinates are problem dependent, however it is the opinion of the authors that some of the linkage can be generalized and the procedure standardized to the point whereby the method can be applicable to a variety of problems without undue difficulty. Total computer costs were shown to be a minor portion of the total effort.

ACKNOWLEDGEMENT

This work was partially supported under a subcontract from General Atomic Co./ETF Design Center.

REFERENCES

1. W. T. Urban, T. J. Seed, and Donald J. Dudziak, "Nucleonic Analyses of the ETF Neutral-Beam-Injector Duct and Vacuum Duct Shields," Los Alamos Scientific Laboratory report to be published.

2. Donald J. Dudziak and P. G. Young, "Review of New Developments in Fusion Nucleonics," Proc. Fourth ANS Topical Meeting Technol. of Controlled Nucl. Fusion, King of Prussia, PA 14-17 October 1980.

3. LASL Group X-6, "MCNP - A General Monte Carlo Code for Neutron and Photon Transport," Los Alamos Scientific Laboratory report LA-7396-M, Revised (1979).

4. T. J. Seed, "TRIDENT-CTR User's Manual," Los Alamos Scientific Laboratory report LA-7396-M, Revised (November 1979).

5. C. I. Baxman and P. G. Young, "Applied Nuclear Data Research and Development January 1 - March 31, 1977," Los Alamos Scientific Laboratory report LA-6893-PR (July 1977).

6. R. E. MacFarlane, private communication from Los Alamos Scientific Laboratory Group T-2 (1980).

7. G. I. Bell, G. E. Hansen, and H. A. Sandmeir, "Multitable Treatments of Anisotropic Scattering in S_N Multigroup Transport Calculations," Nucl. Sci. Eng. 28, 376 (1967).

8. B. G. Carlson, "Tables of Symmetric Equal Weight Quadrature EQ_N Over the Unit Sphere," Los Alamos Scientific Laboratory report LA-4734 (1971).

TABLE I

MCNP/TRIDENT-CTR NBI DUCT COMPARISONS

Region[a]	Quantity	MCNP	TRIDENT-CTR	TRIDENT-CTR / MCNP
I	Flux[b]	3.26+13 (0.0152)[d]	4.19+13[e]	1.29
	Heating[c]	3.60-1 (0.0249)	3.43-1	0.95
II	Flux	1.46+12 (0.0571)	1.83+12	1.25
	Heating	2.19-2 (0.1040)	2.02-2	0.92
III	Flux	1.58+9 (0.0892)	1.54+9	0.97
	Heating	8.80-5 (0.0876)	1.46-4	1.66
IV	Flux[f]	5.45+12 (0.0653)	5.78+12	1.06

a. See Figure 4 for region location
b. Neutron flux, neutrons/cm^2 s
c. Neutron plus gamma-ray heating, MW/m^3
d. Fractional error
e. 4.19+13 = 4.19 x 10^{13}
f. Duct scattered contribution only (see text)

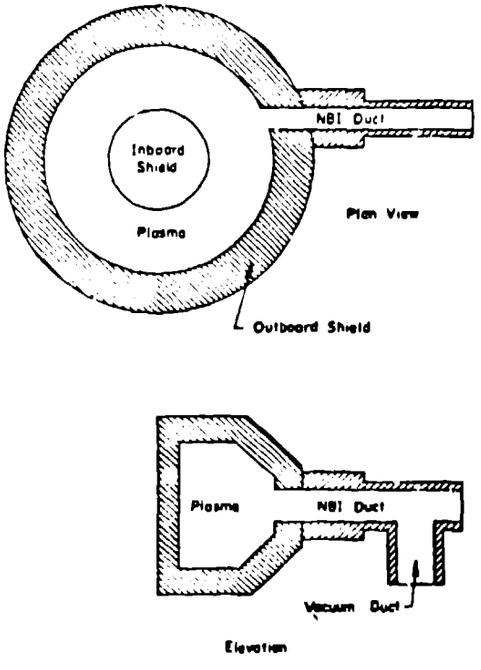

Fig. 1. Schematic of the ETF geometry considered for the MCNP Monte Carlo calculations (not to scale).

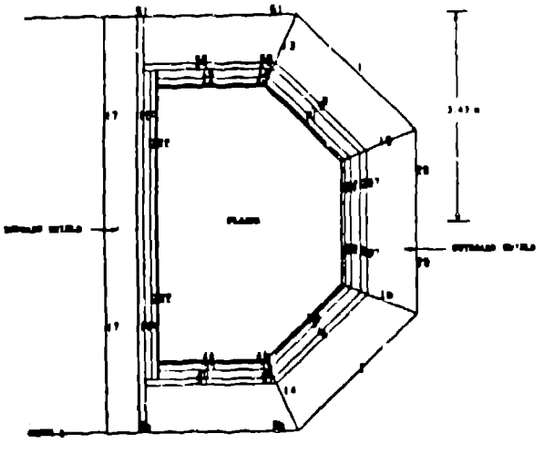

Fig. 2. Elevation cross section through the torus at a toroidal location not including NBI duct, MCNP model.

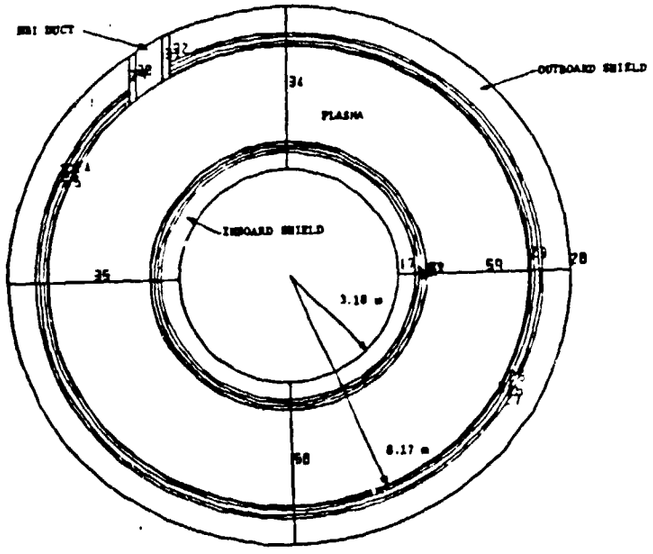

Fig. 3. Plan view at the torus midplane, MCNP model.

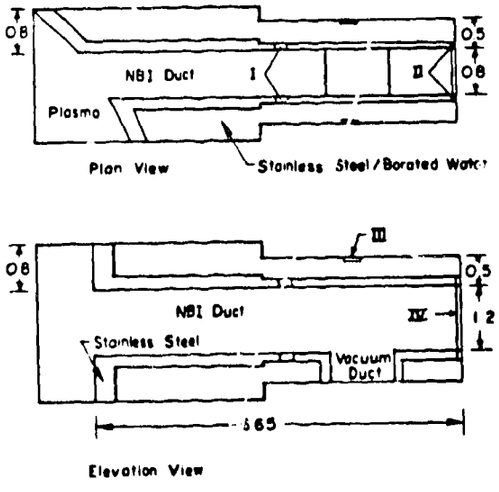

Fig. 4. Plan and elevation views of the MCNP NBI duct model. Dimensions in meters. Roman numerals indicate regions for MCNP/TRIDENT-CTR comparisons.

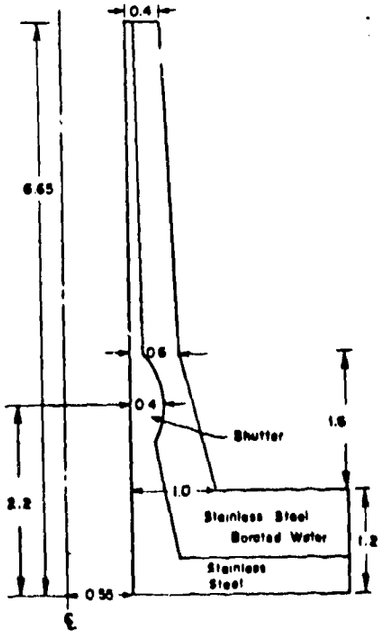

Fig. 5. NBI duct model for TRIDENT-CTR calculations (dimensions in meters).

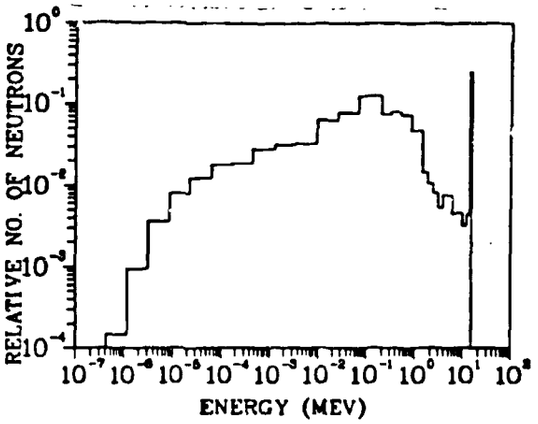

Fig. 6. Energy distribution of neutrons incident on the torus outboard shield at the trapping surface.

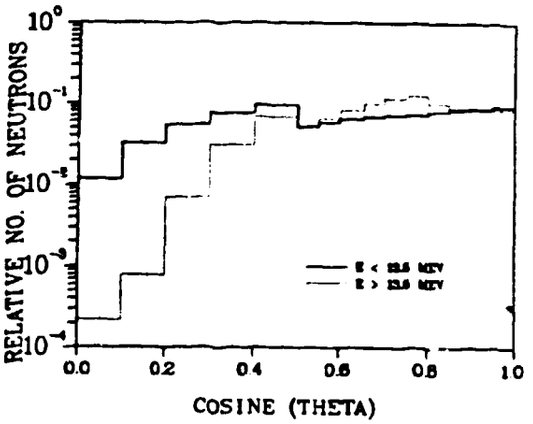

Fig. 7. Angular distribution of neutrons incident on the torus outboard shield at the trapping surface. Theta is the angle between the normal to the trapping surface and the neutron direction.

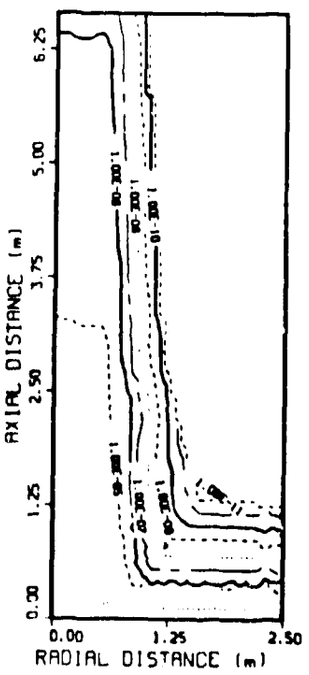

Fig. 8. TRIDENT-CTR NBI duct shield total neutron flux (neutrons/cm^2-s) times 10^{-19}.

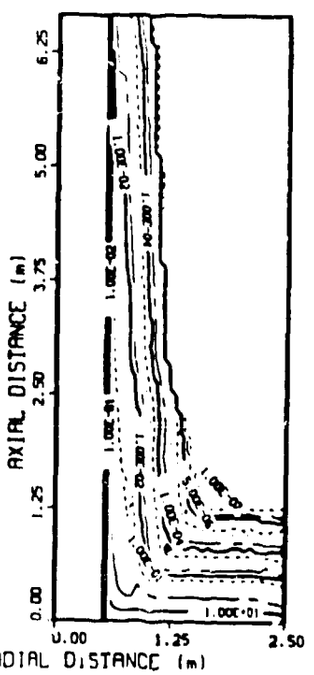

Fig. 9. TRIDENT-CTR NBI duct total (neutron plus gamma-ray) heating (MW/m^3).

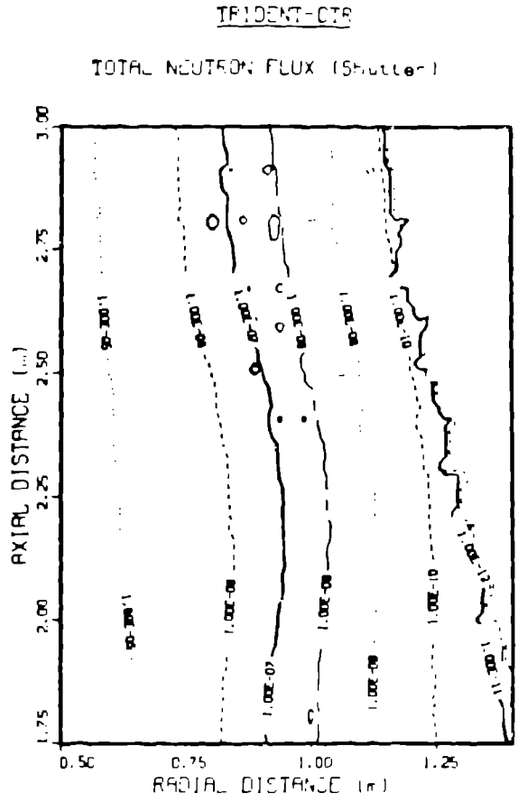

Fig. 10. TRIDENT-CTR total neutron flux (neutrons/cm^2 s) at the shutter shield times 10^{-19}.

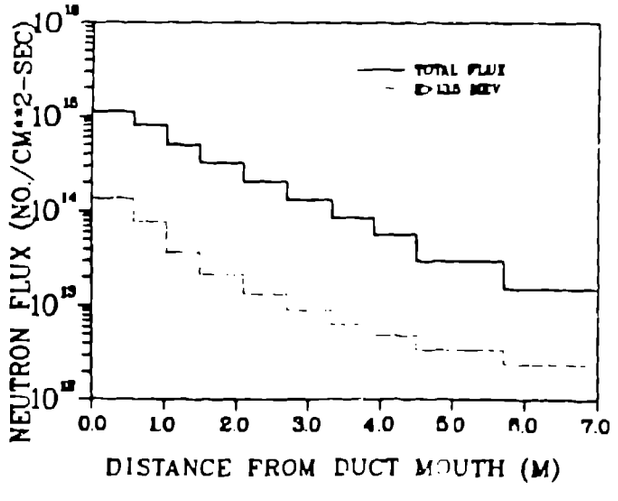

Fig. 11. Neutron flux profile down the NBI duct.